THE JOURNAL OF BIOLOGICAL CHEMISTRY
Vol. 277, No. 43, Issue of October 25, pp. 40832–40838, 2002
Printed in U.S.A.

Formation of Complexes between Ca^{2+}·Calmodulin and the Synapse-associated Protein SAP97 Requires the SH3 Domain-Guanylate Kinase Domain-connecting HOOK Region*

Received for publication, June 6, 2002, and in revised form, August 19, 2002
Published, JBC Papers in Press, August 19, 2002, DOI 10.1074/jbc.M205618200

Ingo Paarmann‡, Oliver Spangenberg‡, Arnon Lavie§, and Manfred Konrad‡¶

From the ‡Department of Molecular Genetics, Max Planck Institute for Biophysical Chemistry, Göttingen D-37070, Germany and the §Department of Biochemistry and Molecular Biology, University of Illinois at Chicago, Chicago, Illinois 60607

Mammalian synapse-associated protein SAP97, a structural and functional homolog of *Drosophila* Dlg, is a membrane-associated guanylate kinase (MAGUK) that is present at pre- and postsynaptic sites as well as in epithelial cell-cell contact sites. It is a multidomain scaffolding protein that shares with other members of the MAGUK protein family a characteristic modular organization composed of three sequential protein interaction motifs known as PDZ domains, followed by an Src homology 3 (SH3) domain, and an enzymatically inactive guanylate kinase (GK)-like domain. Specific binding partners are known for each domain, and different modes of intramolecular interactions have been proposed that particularly involve the SH3 and GK domains and the so-called HOOK region located between these two domains. We identified the HOOK region as a specific site for calmodulin binding and studied the dynamics of complex formation of recombinant calmodulin and SAP97 by surface plasmon resonance spectroscopy. Binding of various SAP97 deletion constructs to immobilized calmodulin was strictly calcium-dependent. From the rate constants of association and dissociation we determined an equilibrium dissociation constant K_d of 122 nM for the association of calcium-saturated calmodulin and a SAP97 fragment, which encompassed the entire SH3-HOOK-GK module. Comparative structure-based sequence analysis of calmodulin binding regions from various target proteins predicts variable affinities for the interaction of calmodulin with members of the MAGUK protein family. Our findings suggest that calmodulin could regulate the intramolecular interaction between the SH3, HOOK, and GK domains of SAP97.

Membrane-associated guanylate kinase homologs (MAGUKs)[1] have been implicated in the assembly of synapses and tight junctions. These are multidomain proteins consisting of one or more PDZ domains, an Src homology 3 (SH3) domain, and a guanylate kinase (GK)-like domain (for reviews, see Refs. 1–4). Rat SAP97 belongs to the MAGUK subfamily comprising *Drosophila* Dlg, SAP97/hDlg, SAP90/PSD-95, SAP102/NE-Dlg, and PSD93/Chapsyn110. SAP97 has earlier been reported to be presynaptic (5), but it has recently been shown also to be present at postsynaptic sites in cerebral cortex (6); it is found both at the post-synaptic density (PSD) region and in the cytoplasm of hippocampal synapses, suggesting a role for SAP97 in ionotropic glutamate receptor trafficking (7). Recently it was discovered that SAP97, via its guanylate kinase (GK)-like domain, directly regulates the function of an inwardly rectifier potassium channel (8). In addition to its crucial role as a scaffolding protein in neuronal cells, SAP97 is an essential component of the basolateral membrane cytoskeleton in a variety of epithelial cells (5).

Each domain in the SAP subfamily of MAGUKs is highly conserved and has been shown to be a site of protein-protein interaction: PDZ domains bind voltage- and ligand-gated ion channels (3, 9); SH3 domains interact with proline-rich, P*XX*PR-like sequences (3, 4, 10) as well as with the GK domain of CASK (11); GKAP/SAPAP (12–14), the microtubule-associated protein MAP1A (15), the brain-enriched guanylate kinase associated protein (BEGAIN) (16), and the guanylate kinase associated kinesin GAKIN (17) are interaction partners of the GK domain. The GK domain is catalytically inactive, although structurally closely related to authentic guanylate kinases as we have shown in previous work (18, 19).

Despite striking overall structural similarities of SAP family members, these proteins associate with their binding partners by specific mechanisms: first, subtle variations in the sequences flanking the conserved PDZ, SH3, and GK domains have been shown to be responsible for the differential localization of these proteins (20), and second, intramolecular as well as competing intermolecular interactions of the individual domains may regulate the association of specific binding partners (15, 21). Notably, SAP97 sequences located N-terminal to the first PDZ domain were found essential for multimerization (22), and the U5 region, also called the HOOK domain, which is located between the SH3 and GK domains, was reported to contain an actin binding protein 4.1 binding site in the alternative I3 splice variant (23) as well as a putative calmodulin (CaM) binding site (24). By searching in the SAP97 HOOK domain for potential CaM binding sites that conform to the proposed motifs of charge, hydrophobicity, and amphiphilicity distribution in CaM binding peptides and proteins (25, 26), we identified key residues that are predicted to anchor this region to the N- and C-terminal domains of CaM.

Because the SH3 and the GK domains of MAGUKs show both intramolecular and intermolecular interactions (11, 27–

* This work was supported by Research Grant RG 0120/1999-B of the Human Frontier Science Program (to I. P., A. L., and M. K.), by the Deutsche Forschungsgemeinschaft, and by the Max Planck Society (to O. S. and M. K.). The costs of publication of this article were defrayed in part by the payment of page charges. This article must therefore be hereby marked "*advertisement*" in accordance with 18 U.S.C. Section 1734 solely to indicate this fact.

¶ To whom correspondence should be addressed. Tel.: 49-551-201-1706; Fax: 49-551-201-1718; E-mail: mkonrad@gwdg.de.

[1] The abbreviations used are: MAGUK, membrane-associated guanylate kinase homolog; CaM, calmodulin; GST, glutathione *S*-transferase; GKAP, guanylate kinase-like domain associated protein; SAP, synapse-associated protein; PSD, post-synaptic density; GAKIN, guanylate kinase associated kinesin; BEGAIN, brain-enriched guanylate kinase associated protein; Dlg, discs-large; SAPAP, SAP-associated protein; MAP1A, microtubule-associated protein 1A; SPR, surface plasmon resonance; SH3, Src homology 3; RU, resonance unit(s).

29), CaM binding to these sites may modulate the scaffolding properties of SAP97 by affecting the equilibrium between intra- and intermolecular assembly. In fact, a CaM-dependent clustering of *N*-methyl-D-aspartic acid receptors by heteromeric MAGUK protein complexes has been proposed (24), and a pivotal role has been attributed to SAP97 as a major constituent of a membrane-anchoring complex that contains Ca^{2+}/calmodulin-dependent protein kinase II, actin, actinin, and protein 4.1 (30). This view has been strengthened by recent mass spectrometric identification of these proteins in large postsynaptic density complexes (31, 32). In the present study, using surface plasmon resonance (SPR) spectroscopy, we have analyzed the structural features required for the molecular interaction between SAP97 and CaM. Our results show that CaM binding to SAP97 occurs at the HOOK domain and that the HOOK domain-GK domain module is sufficient for CaM binding, but the presence of an intact SH3 domain promotes CaM binding, in a strictly calcium-dependent manner. Our findings suggest that calmodulin acts as a trigger for the opening and closing of the SAP97 molecule via a mechanism, which may allow this multidomain protein to differentially associate with various binding partners.

EXPERIMENTAL PROCEDURES

Cloning of CaM and Generation of SAP97 Mutants—CaM was amplified from a human cDNA library (Invitrogen) using the following pair of primers: 5′-GGAATTC*CATATG*GCTGACCAACTGACTGA-3′ (sense primer, introducing an *Nde*I restriction site) and 5′-CGGGATCCTCACTTTGCTGTCATCATTTG-3′ (antisense primer, introducing a *Bam*HI site). The SAP97 cDNA clone was a generous gift of C. C. Garner, Department of Neurobiology, University of Alabama at Birmingham, Birmingham, AL. The intrinsic *Bam*HI site in the GK domain of SAP97 was removed by PCR-based site-directed mutagenesis using the following primer pairs (location of the mutated site shown in italics): 5′-CCTGACAAATTT*GGCAGC*TGTGTCCCTC-3′ (sense), 5′-GAGGGACACA*GCTGCC*AAATTTGTCAGG-3′ (antisense). The SAP97 N-terminal deletion constructs (as illustrated in Fig. 1*A*) were generated using the following sense primers (*Nde*I and *Bam*HI restriction sites underlined): 5′-GGAATTCCATATGCTCCGAACCAGCCAAAAG-3′ (SAP97-1), 5′-GGAATTCCATATGGTTGGAGTAATTCCTAGTA-3′ (SAP97-2), 5′-GGAATTCCATATGTCATTCAATGACAAGCGTA-3′ (SAP97-3), 5′-GGAATTCCATATGACCCGACCAGTCATCATATTAG-3′ (SAP97-4), 5′-GGAATTCCATATGTCAAAAGGTGGTCAAGAAGAATA-3′ (SAP97-5), and the following antisense primers: 5′-CGGGATCCTCATAATTTTTCTTTTGCTGGGA-3′ (SAP97-1 to SAP97-5), 5′-CGGGATCCAGACTGCTCTTCTATGATCTGCTT-3′ (SAP97-6), 5′-CGGGATCCTCACCCTTTATCTCCTCTTGTTTTAG-3′ (SAP97-7), and 5′-CGGGATCCTCATTCGTCACTCTCACCATCTG-3′ (SAP97-8). All PCR fragments were cloned as *Nde*I-*Bam*HI-restricted fragments. The dlg^{m30} (L612P) mutation (33) was introduced via site-directed mutagenesis using the primer pair: 5′-GGAGATATT*CCC*CATGTTATCAATGCTTC-3′ (sense; mutated site shown in italics), 5′-GAAGCATTGATAACATG*GGG*AATATCTCC-3′ (antisense). All constructs were ligated into a modified pGEX-2T expression plasmid described elsewhere (34) and were verified by automatic DNA sequencing (Applied Biosystems 373 Sequencer) and data analysis to confirm clone integrity.

Protein Purification—All proteins were produced as GST fusion proteins in *Escherichia coli* BL21(DE3) CodonPlus strain (Novagen). Expression of the recombinant proteins was induced with 0.2 mM isopropyl-1-thio-β-D-galactopyranoside at 25 °C overnight. Bacteria were lysed by sonication. Applying the manufacturer's standard protocol (Amersham Biosciences), the cleared lysates were passed over a glutathione-Sepharose column. After extensive washing with phosphate-buffered saline, the proteins were eluted as GST fusion proteins, or cleaved from the beads with thrombin at 4 °C overnight. Protein concentration was determined at 280 nm using specific extinction coefficients (units of cm^2mg^{-1}) that were calculated from the amino acid composition according to (35): 0.85 for SAP97-1, 0.62 for SAP97-2, 0.69 for SAP97-3, 0.73 for SAP97-4, and 0.65 for SAP97-5.

Surface Plasmon Resonance Measurements—Association and dissociation reactions of calmodulin and SAP97 fragments were performed by surface plasmon resonance (SPR) spectroscopy using a BIAcore 2000 system (BIAcore AB, Uppsala, Sweden). Calmodulin, referred to as the ligand, was immobilized on a sensor chip, and the interaction with SAP97 fragments free in solution, referred to as the analyte, was detected through mass concentration-dependent changes of the refractive index on the sensor surface (for a review of kinetic analyses using the SPR technique, see Ref. 36). All of the reagents such as an amine coupling kit, surfactant P-20, and the CM-5 sensor chip were purchased from BIAcore AB. Four flow cells were placed in a CM-5 sensor chip surface. Using a GST fusion capture kit (BIAcore), anti-GST antibody was immobilized on all flow cells according to the manufacturer's instructions. GST-tagged CaM was then captured in one flow cell. GST protein alone was captured in a different flow cell, which served for on-line reference subtraction. The running buffer for all experiments, except for determination of the Ca^{2+} dependence of calmodulin binding, was composed of 10 mM $CaCl_2$, 10 mM dithiothreitol, 10 mM HEPES, pH 7.4, 0.15 M NaCl, 3.4 mM EDTA, and 0.05% surfactant P-20. For Ca^{2+} dependence experiments, 10–300 μM $CaCl_2$, 10 mM dithiothreitol, 10 mM HEPES, pH 7.4, 0.15 M NaCl, 1 mM $MgCl_2$, and 0.05% surfactant P-20 were used as running buffer. Captured GST-CaM was regenerated in 1 M NaCl. Anti-GST antibody on the CM5 surface was regenerated according to the GST fusion kit manual using 1-min pulses of 10 mM glycine, pH 2.2, at flow rates of 10 μl/min. All solutions used for SPR measurements were filtered (0.22 μm) and degassed.

The changes in the observed SPR signal are expressed as resonance units (RU). A response change of 1000 RU corresponds to a change in the surface concentration of about 1 ng of protein per mm^2 on the sensor chip (50). Rate constants for the association and dissociation of free analyte (*A*) to sensor chip-bound ligand were calculated using the BIAevaluation 3.1 software. Control experiments using varying ligand densities on the sensor chip (resulting in 300–1500 RU) and flow rates of the analyte (between 5 and 30 μl/min) were performed to detect mass transfer-limited interactions that might affect kinetic analysis (36). To determine rate constants of association and dissociation, kinetic measurements were performed at a flow rate of 30 μl/min and by adjusting the immobilization level of captured GST-CaM to 300–500 RU. The apparent binding rate under mass transfer-limiting conditions was calculated from the linear part of the association phase using a flow rate of 5 μl/min and 1300 RU of captured GST-CaM ligand. For competition experiments, varying amounts of untagged CaM were co-injected with 0.5 μM SAP97-1, and the binding rate was determined.

Assuming a one-to-one binding model without mass transfer, the association reaction was analyzed according to the equation, $R_t = \{k_a[A]R_{max}/(k_a[A] + k_d)\}\,[1 - e^{-(k_a[A]+k_d)t}]$. Here, R is the time-dependent SPR signal, $[A]$ the concentration of the injected analyte, k_a the association rate constant, and k_d the dissociation rate constant. Under conditions where $k_a[A]$ is much greater than k_d, this equation simplifies to: $R_t = R_{max}\,[1 - e^{-(k_a[A]+k_d)t}]$. The observed rate, k_{obs}, is then linearly dependent upon the concentration of the analyte: $k_{obs} = k_a[A] + k_d$. The dissociation phase can be described by $R_t = R_0\, e^{-k_d(t-t_0)}$, assuming that the rebinding of released analyte is negligible, where R_t is the response at time t and R_0 the signal at an arbitrary starting point t_0. With the rate constants determined by a series of analyte concentrations, the dissociation constants were calculated according to $K_d = k_d/k_a$.

RESULTS

Expression of Recombinant SAP97 C-terminal Fragments—GST fusion proteins of SAP97 constructs were expressed in *E. coli* BL21-CodonPlus and purified over a GSH-Sepharose column. The GST moiety was removed by thrombin cleavage, yielding >95% pure proteins. Because it proved to be difficult to overproduce full-length SAP97 (925 amino acid residues) in bacteria, we first generated a 350-residue fragment (construct SAP97-1), which encompassed the entire SH3 domain, the HOOK/U5 region, and the GK domain, including the 12-residue C terminus. To map the putative CaM binding domain and to determine the sequence motifs for specific SAP97 binding, we successively deleted the SH3 domain, the first part of the U5 region, the I3 insert, and the region between the I3 insert and the GK domain (Fig. 1*A*). Recombinant proteins that contained the SH3 domain, but lacked the C terminus (constructs SAP97-6, -7, and -8) tended to form inclusion bodies upon bacterial expression and were not analyzed further.

Structural Elements of SAP97 Required for CaM Binding—As an approach for quantifying the dynamic parameters of the SAP97-calmodulin interaction, we used surface plasmon resonance (SPR) spectroscopy, which allowed us to directly observe the binding of SAP97 fragments that immobilize GST-

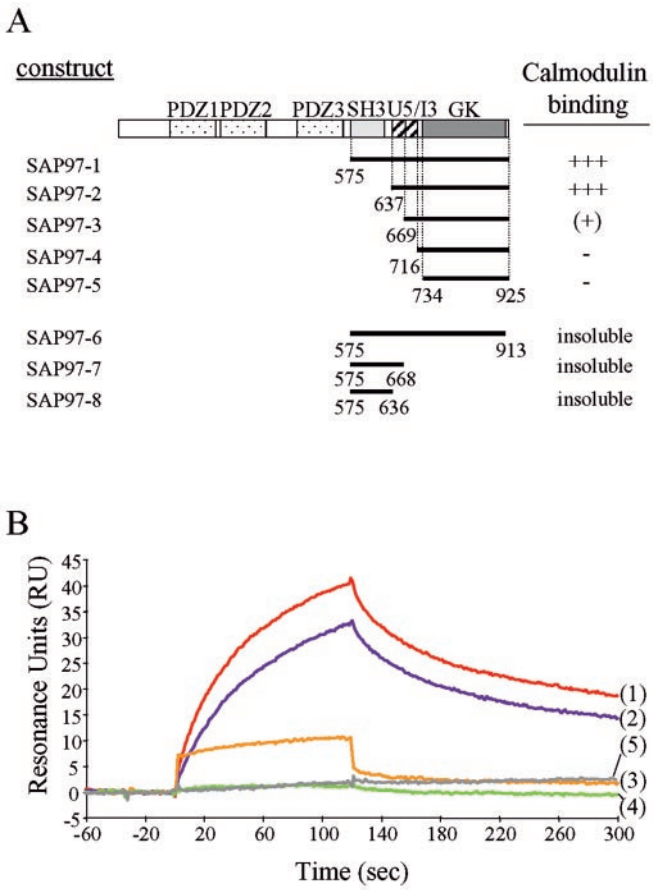

FIG. 1. **Localization of the calmodulin binding site in SAP97.** *A*, schematic presentation of SAP97 deletion constructs. Depicted at the *top* is the domain structure of SAP97 consisting of three PDZ domains, the SH3, and the GK domain; also labeled is the U5 region, including the alternatively spliced I3 insert. The *numbers* indicated for each construct correspond to the positions of the first and the last amino acid, respectively, in the full-length protein. In the *right column*, the CaM binding properties are summarized for each construct. +++, strong binding; (+), very weak binding; −, no binding detected. *B*, surface plasmon resonance analysis to detect interaction between the five SAP97 constructs that were obtained as soluble proteins. Captured GST-CaM was used as ligand. All constructs were applied at 1 μM. Injection started at 0 s and was stopped after 120 s.

calmodulin (GST-CaM) and to assess parameters of binding and dissociation kinetics. To immobilize GST-CaM we used a sandwich assay with anti-GST polyclonal antibodies covalently bound via amine coupling to the carboxylated dextran matrix of the sensor chip surface. We observed that the GST fusion protein bound in this way was fixed to the surface matrix in a nearly irreversible manner. Regeneration with 10 mM glycine, pH 2.2, resulted in complete dissociation of all non-covalently bound ligands, whereas the immobilized antibodies retained almost full binding activity. To screen for the relative affinity of SAP97 fragments to GST-CaM, a single sensor chip was used to detect binding at 1 μM analyte concentration. Fig. 1*B* represents GST-CaM interaction analysis of SAP97 fragments that contain the entire GK domain and adjacent N-terminal regions of variable lengths. Construct SAP97-1, which contains the SH3 domain, shows the strongest interaction; construct SAP97-2, which is devoid of the SH3 domain, has about a 3-fold reduced binding affinity (Table I), whereas deletion of both the SH3 domain and the N-terminal half of the U5 region in SAP97-3 leads to an almost inactive protein in this binding assay. The even shorter fragments SAP97-4 and SAP97-5 showed no interaction, thus highlighting the intact U5 region as an essential structural element for binding of calmodulin.

TABLE I
Characteristics of CaM interaction with SAP97 constructs

The kinetic characteristics of the interaction with CaM determined for different SAP97 constructs are summarized (see Fig. 1). Association rate constants (k_a), dissociation rate constants (k_d), and equilibrium dissociation constants ($K_d = k_d/k_a$) are given.

Construct	k_a	k_d	K_d
	1/mM·s	*1/min*	*nM*
SAP97–1	19.9 ± 8.3	0.16 ± 0.10	122 ± 46
SAP97–1(L612P)	7.5 ± 2.3	0.14 ± 0.04	328 ± 76
SAP97–2	10.8 ± 2.3	0.20 ± 0.05	334 ± 141
SAP97–3	ND[a]	ND	Weak binding
SAP97–4	−[b]	−	No binding
SAP97–5	−	−	No binding

[a] ND, not determined.
[b] −, not binding detectable.

Kinetics of the Interaction between SAP97 and Calmodulin—In initial experiments, the specificity of the interaction of SAP97 with CaM was evaluated by testing the SAP97-2 fragment for binding to immobilized CaM. Sensorgrams of the association phase were recorded at SAP97-2 concentrations varying from 0 to 500 nM in the running buffer (Fig. 2*A*). The apparent binding rate increased linearly in the entire concentration range (Fig. 2*B*). To ensure that fragment SAP97-2 bound in the target site of CaM and did not simply show a nonspecific interaction with CaM and to find out whether steric hindrance in protein-protein interaction may become critical when using the SPR technique, we performed competition experiments with soluble, untagged calmodulin. To this end, 0.5 μM SAP97-2 was preincubated with CaM in the 0.25–7.5 μM concentration range for at least 15 min before injection into the flow cell. Monophasic association was observed, with the amplitude of the SPR signal nearly vanishing at the highest concentration chosen. Fig. 2*C* shows that surface-bound CaM efficiently competes with free CaM for interaction with SAP97, the apparent EC_{50} value being about 2 μM.

To quantify the interaction of SAP97 with calmodulin as well as to determine comparative values for a presumed interaction of other MAGUKs, we performed surface plasmon resonance measurements using immobilized GST-CaM and purified SAP97-1 protein, which encompasses the SH3, U5, and GK domains. The interaction was studied in real-time as a function of SAP97-1 concentration. Fig. 3*A* shows *traces* of the change in mass (resonance units) on the sensor chip surface upon passing increasing concentrations of SAP97-1 over the antibody-fixed GST-CaM ligand. Analysis of the association and dissociation phases of the sensorgrams yielded an association rate constant, k_a, of 2×10^4 $M^{-1}s^{-1}$, and a dissociation rate constant of 2.6×10^{-3} s^{-1}. The calculated dissociation equilibrium constant, K_d, of 1.3×10^{-7} M is indicative of a low to intermediate affinity complex of calmodulin (37) and SAP97. The association rate constant is fairly low for a one-to-one reaction type, although it is very similar to the value reported for neuronal and endocrine dlg (NE-dlg) interaction with calmodulin (24). The results of the kinetic analysis performed on all five SAP97 deletion constructs as well as on the SAP97-1(L612P) mutant protein are summarized in Table I.

Calcium Dependence of Calmodulin Binding to SAP97—A number of target proteins bind to Ca^{2+}-free calmodulin or the affinity of CaM-protein complexes may be quantitatively modulated depending on the extent of calcium saturation of calmodulin (38). Therefore, we were interested in answering the question of whether the association of SAP97 is calcium-regulated. When $CaCl_2$ was varied from 10 to 300 μM, in the presence of 150 mM NaCl, 1 mM $MgCl_2$, without EDTA, we observed that binding of the SAP97-1 protein was only weakly affected at concentrations above 30 μM $CaCl_2$, whereas it was hardly detect-

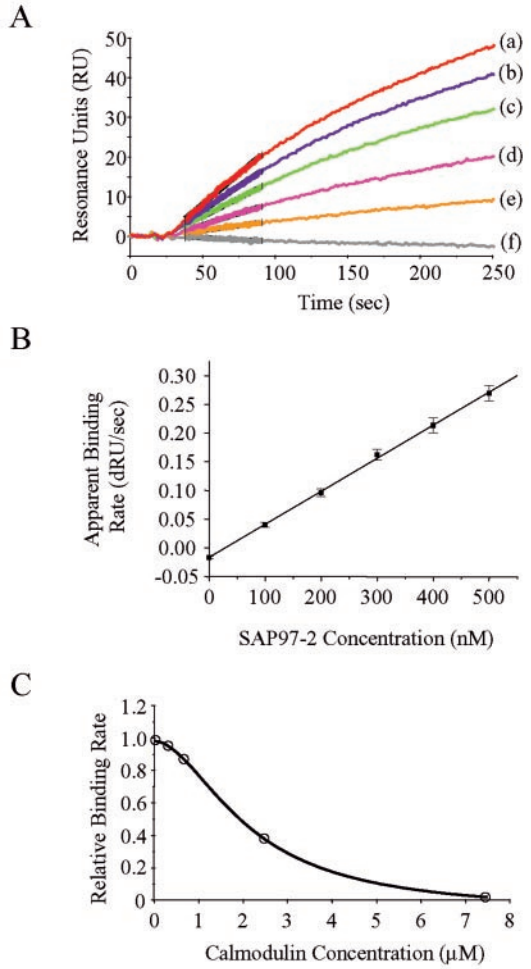

FIG. 2. **Specific association of SAP97 and CaM.** *A*, real-time interaction analysis of SAP97-2 binding to sensor chip-coupled GST-CaM. Sensorgrams of the association phase were recorded using different amounts of construct SAP97-2: *a*, 500 nM; *b*, 400 nM; *c*, 300 nM; *d*, 200 nM; *e*, 100 nM; *f*, 0 nM. The injection of protein started at time point 25 s. The *boldface* areas were used for the calculation of initial rates using BIAEvaluation 3.1 software. *B*, the apparent binding rates of SAP97-2 were calculated from each sensorgram shown in *A* and are plotted as a function of the protein concentration; each data point represents the average of four independent experiments. *C*, competitive inhibition of the interaction between captured GST-CaM and SAP97-2 by soluble CaM. SAP97-2 (0.5 μM) was incubated with free CaM at concentrations from 0 to 7.5 μM. The binding rates were determined as in *A*. To normalize binding rates, all rates were divided by the binding rate at 0 μM free CaM.

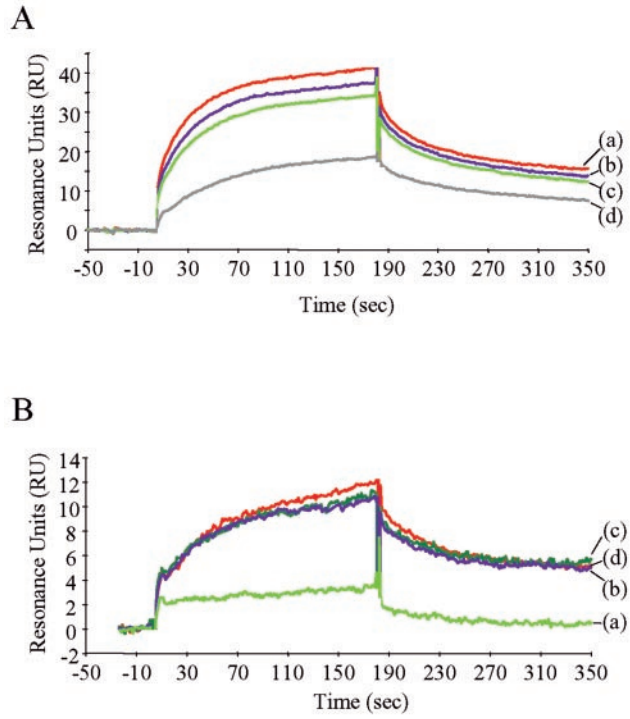

FIG. 3. **Determination of the dissociation constant for the interaction between SAP97-1 and CaM.** *A*, the interaction kinetics between CaM and SAP97 were measured in the presence of 10 mM Ca^{2+} and 0 mM Mg^{2+} by passing different concentrations (*a*, 1 μM; *b*, 0.75 μM; *c*, 0.5 μM; *d*, 0.25 μM) of purified SAP97-1 protein over the immobilized GST-CaM. Injection of SAP97-1 started at 0 s and was stopped at 180 s. The dissociation phase was recorded by flushing the flow cell without SAP97-1. The rate constants (k_a, k_d) were determined from the association and dissociation phases using a curve fitting program. A monophasic one-step, bi-molecular association model was sufficient to fit the sensorgrams. The equilibrium dissociation constant, K_d, was calculated according to $K_d = k_d/k_a$. *B*, the calcium dependence of the SAP97-CaM interaction was determined at 10 μM (*a*), 30 μM (*b*), 100 μM (*c*), and 300 μM Ca^{2+} (*d*) in the presence of 1 mM Mg^{2+}. Sensorgrams were recorded by using 0.5 μM SAP97-1 and are shown as overlay.

able at 10 μM (Fig. 3*B*). The calculated dissociation constants were 124 ± 62 nM at 30 μM, 113 ± 24 nM at 100 μM, and 171 ± 35 nM at 300 μM Ca^{2+}; no binding was detected at 10 μM Ca^{2+}. Under these conditions, which are in the physiological range of ionic strength and Mg^{2+} concentration, the Ca^{2+}·CaM complex has an overall apparent dissociation constant of ~10 μM (39). It can be expected that, despite a direct competition between Ca^{2+} and Mg^{2+} binding for the four Ca^{2+} binding sites (40), CaM reaches the Ca^{2+}-saturated state at 30 μM Ca^{2+}, implying that it is the $(Ca^{2+})_4$·CaM species that associates with SAP97.

Role of the SH3 Domain for CaM-SAP97 Interaction—Our kinetic data suggest that the SH3 domain provides little binding energy for complex formation between SAP97 and calmodulin, because the affinity of the SAP97-3 fragment, which lacks the SH3 domain, was only 3-fold weaker than that of the wild-type SAP97-1 construct (Table I). This relatively small, but reproducibly observed differential effect appears to be due to a slight decrease of the association rate constant and a slight increase of the dissociation rate constant. We also tested whether calmodulin association was affected by a leucine-to-proline point mutation in the SH3 domain of SAP97, SAP97(L612P). This leucine residue is conserved among MAGUK family members, and L612P corresponds to a point mutation that was first identified in the *Drosophila dlg* gene (*dlg*^{m30} allele; L632P mutation) where it produced a strong phenotype associated with loss of normal cell proliferation control (33). Moreover, the equivalent L460P mutation in the PSD-95 protein has been shown to interrupt intramolecular interaction between the SH3 and GK domains (27, 28). The data we obtained for the SAP97(L612P) protein were very similar to those of the SH3-free protein (SAP97-2 construct), suggesting that calmodulin most efficiently binds to the intact protein in which intramolecular association of the SH3 and GK domains can occur.

SAP97 Sequence Motifs for Calmodulin Recognition—To understand the structural basis for SAP97-calmodulin interaction, we analyzed the HOOK domain for sequence motifs known to be engaged in calmodulin recognition (26, 41). Fig. 4*B* presents an alignment of amino acid sequences from putative CaM-binding regions of five MAGUKs in comparison with CaM-binding domains of selected target proteins that were shown to bind CaM in a Ca^{2+}-dependent manner. This subclass of CaM-binding proteins contains the so-called 1-8-14 binding motif, which designates the position of conserved hydrophobic/aromatic residues that anchor the target protein to the two lobes of Ca^{2+}·CaM (26). SAP97 and its relatives conform to this

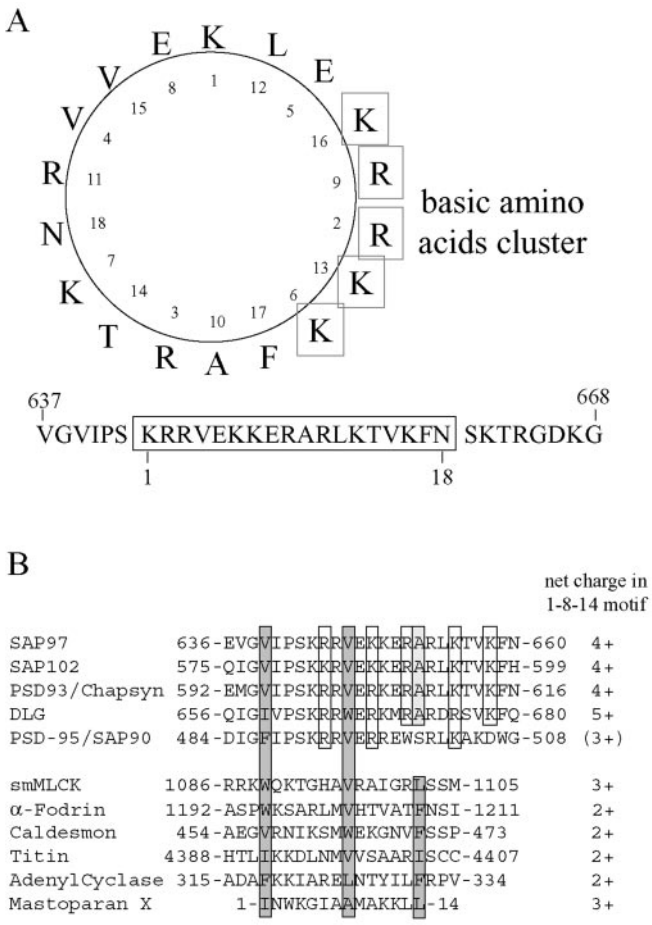

FIG. 4. **Primary structure analysis of the CaM-binding sites from SAP97 and various target proteins.** *A*, helical wheel representation of the putative 18-residue CaM-binding region from SAP97. The *numbers within the circular plot* indicate the positions of the residues in the linear sequence. Basic residues that cluster to one side of the wheel are *boxed*. This is not a perfect amphipathic α-helix because polar residues are also found on the opposite side. *Below* is shown the complete sequence that is critical for CaM binding according to the interaction analysis of CaM with SAP97 deletion constructs. The CaM binding was located in the region that starts at position 637 and ends at position 668. The part depicted as the helical wheel is *boxed*. *B*, amino acid sequence alignment of the CaM binding site of SAP97 and homolog regions of four other members of the SAP97 subfamily of MAGUKs, in comparison to CaM binding domains identified in various target proteins and peptides showing the 1-8-14 type B CaM binding motif. *Boxed* are the residues of the basic amino acids cluster of the MAGUK proteins, and *highlighted* in *dark gray* are the hydrophobic amino acids of this CaM binding motif; the alanine residue at the position corresponding to the last amino acid of the 1-8-14 motif is shown in *light gray*. In the *right column*, the net charge of the region between the first and the last amino acid of the motif is indicated.

1-8-14 pattern of characteristic CaM binding residues and of net electrostatic charges of +3 to +5 within this motif. In addition, this motif (SAP97 residues 639–652) is situated in an α-helix that covers SAP97 residues 643–660, being equivalent to PSD-95 helix α1 (residues 491–508), which was recognized in the crystal structure of the PSD-95 SH3-GK fragment as a prominent structural element showing high conformational variability (29). A helical wheel representation of this 18-residue helix in SAP97 (Fig. 4*A*) shows clustering of five positively charged residues on one side, thus demonstrating that both hydrophobic and electrostatic interactions contribute to binding of the SAP97 HOOK domain, which we identified as a CaM recognition region.

DISCUSSION

Understanding molecular mechanisms that govern complex macromolecular interactions is one of the major goals of structural biology. The interactions between the SAP97/hDlg multidomain protein, a member of the MAGUK protein family, and its putative binding partners have so far only been studied by qualitative or at best semi-quantitative cell biological methods using the yeast two-hybrid approach or co-immunoprecipitation techniques for detecting protein-protein association (21, 42). Detailed studies of tertiary structures of MAGUKs have been confined to the C-terminal half of SAP90/PSD95 encompassing the SH3, HOOK, and GK domains (29, 43), and our most recent work on human CASK has revealed distinctive structural features of the CASK GK binding module in comparison to enzymatically active guanylate kinase (19). However, no complex between a MAGUK and any interacting protein has been crystallized so far. Because SAP97 is one of the main players in the postsynaptic density network, acting as scaffolding or clustering protein for various membrane receptors and transporters and linking regulatory and signaling proteins to the membrane cytoskeleton and to signal transduction pathways, we commenced a detailed structural analysis of its interaction with calmodulin, which we identified as an SAP97 binding partner. In the present study, we have used purified proteins to analyze calcium-dependent association of human calmodulin and rat SAP97.

The CaM Binding Site Is Located in the HOOK Domain—We note that SAP97 interacts with CaM mainly in the so-called U5, or HOOK, region, which connects the SH3 and GK domains. The homologous region of SAP102 has also been shown to bind CaM (24). Representation of the critical 18 residues region as a helical wheel (Fig. 4*A*) reveals a cluster of basic amino acids having a calculated net charge of +4. The characteristic amphiphilic helix-CaM interaction motif (25, 44) that encompasses a series of hydrophobic amino acids lying opposite to the basic amino acid cluster in such a helix is virtually absent in SAP97, explaining the three orders of magnitude weaker CaM binding compared with model peptides (25). However, three further, non-canonical Ca^{2+}-dependent CaM binding motifs have recently been proposed (26). These motifs consist of hydrophobic amino acids occurring at positions 1-8-14, 1-5-8-14, or 1-5-10 and have a net charge of +2 to +6 within the CaM binding region. At first glance, none of these three motifs appears to fit to SAP97, because hydrophobic amino acids are found only at positions 1 and 8 (see Fig. 4*B*), and an alanine residue is located at position 14. Inclusion of alanine in the group of allowed amino acids at position 14, the U5 region of SAP97 fulfills all criteria for a typical 1-8-14 type B CaM recruitment motif. The significantly higher affinity of CaM to SAP97 as compared with caldesmon ($K_d \sim 1$ μM (45)) and α-fodrin/brain spectrin ($K_d \sim 3$ μM (46)), which also have the 1-8-14 type B motif, may result from the higher net charge (+4 for SAP97 as compared with +2 for the latter two proteins). Our primary structure analysis highlights eight residues important for CaM association: a modified 1-8-14 binding motif and the basic amino acid cluster. These eight residues are not only present in SAP97 and SAP102 but are also found in PSD93/chapsyn and discs-large (DLG), suggesting that other members of the MAGUK protein family might form complexes with CaM with similar affinity. In SAP90/PSD-95, three of the eight key residues are missing, resulting in a lower net charge in the critical binding region. Therefore, SAP90 is predicted to bind CaM with lower affinity as compared with SAP97; this is in line with preliminary data we obtained from the kinetic analysis of the CaM-SAP90 interaction.[2]

[2] I. Paarmann and M. Konrad, unpublished data.

It is noteworthy that sequences on both sides of the critical region affect CaM binding. First, our results indicate that CaM weakly binds to the I3 insert as well. This may be due to electrostatic interactions with the set of eight basic amino acids located in the stretch of twenty residues that follow the critical region. Second, the presence of the SH3 domain significantly increases the affinity. From these observations we may assume that the "closed," cis-interacting conformation of the SH3-GK region (21, 29, 43) could prevent binding of ligands to the SH3 domain and/or to the GK domain. The binding of high affinity ligands such as CaM is thought to "open" the compact, intramolecularly stabilized SH3-HOOK-GK region and allow access of proteins to the GK domain (28). This view is in line with the inhibitory effect of the SH3 domain on the interaction of the GK domain with GKAP, which was already described (21), and it is reminiscent of the regulation mode of Src family tyrosine kinases (47). Because we found preferential binding of CaM to the closed conformation of the SH3-GK region, it is unlikely that CaM is involved in the "unfolding" of the SH3-GK region. Using spectroscopic and hydrodynamic techniques we are now attempting to reveal whether CaM induces conformational transitions and domain re-arrangements in the SH3-HOOK-GK module that stabilize a more extended fold of the molecule, thereby unmasking binding sites for GKAP association.

Role of the C-terminal Tail—At present, no quantitative data are available on the postulated dynamic equilibrium between open and closed conformations in SAP97 (21) and SAP90 (43). Remarkably, the last 12 residues C-terminal to the GK domain of SAP90 appear to play a critical role in forming the native conformation of the molecule (29), because they were shown to fold into a β-strand that actually is a structural component of the SH3 domain formed through three-dimensional domain swapping (43). Sequence comparison predicts very similar secondary structural elements for the SH3-HOOK-GK module of SAP97 (29), suggesting that most residues of the C-terminal β-strand are involved in hydrophobic interactions with residues from the SH3 and HOOK domains. These structural constraints may explain why we were unable to produce in soluble form the SH3-HOOK-GK module of SAP97 without the 12 C-terminal residues; this construct was expected to show a weakened, or even interrupted, intramolecular association between the GK and SH3 domains.

A simple bimolecular one-step association model was sufficient to fit the sensorgrams, and no significant change in kinetic constants was observed when the flow rate of the SAP97 proteins was increased 6-fold. Also, association and dissociation rate constants were not influenced by a 5-fold variation in the amount of immobilized CaM. Though kinetic data obtained from SPR measurements have the advantage of working with a label-free system, immobilization of the protein analyte could influence the binding kinetics through restricted mobility of the binding sites. Because the second order rate constants determined here are at least two orders of magnitude lower than those expected for a diffusion-controlled reaction, binding of SAP97 to CaM could involve formation of a recognition complex that subsequently isomerizes to the final complex. Experimental limitations of the SPR technique prevented the use of much higher SAP97 concentrations to eventually detect upper limits of the observed association rates. However, using isothermal titration microcalorimetry, we were able to determine a 1:1 molar ratio for complex formation between SAP97-1 and calcium-saturated CaM.[2]

Calcium-dependent Interaction between CaM and SAP97—Calmodulin, the small, highly acidic (net charge of −17 after being complexed with four Ca^{2+} ions) calcium binding protein of 148 amino acid residues, is the principal mediator of calcium-dependent signaling in eukaryotic cells, regulating the activities of a large number of different target proteins (41). Its activity strongly depends on the intracellular free Ca^{2+} concentration, which transiently increases from less than 0.1 μM in a resting cell to 1–10 μM in an activated cell, whereas the Mg^{2+} concentration remains nearly constant at 0.5–2 mM (48). The competition of Mg^{2+} and Ca^{2+} for binding to the same sites has significant effects on the population of Ca^{2+}-loaded states of CaM. Ca^{2+} binds to the two high affinity C-terminal sites ($K_d \sim 1$ μM) and the two low affinity N-terminal sites ($K_d \sim 10$ μM) in a cooperative manner, and the apparent Ca^{2+} affinity increases upon binding of CaM to a target molecule (40). Our experiments on Ca^{2+} dependence of CaM-SAP97 association showed that at 10 μM Ca^{2+} the interaction was hardly detectable, whereas 30 μM Ca^{2+} in the presence of 1 mM Mg^{2+} was sufficient for obtaining full binding activity. Thus, our kinetic data directly confirm the Ca^{2+}-saturated CaM species as the binding partner for SAP97.

Efficient activation of low affinity CaM targets ($K_d > 100$ nM) such as SAP97 occurs only where free Ca^{2+}-activated CaM concentrations can be locally increased (37). Because synapse development is dependent upon neural activity (49), the associated Ca^{2+} influx might induce such a local increase in Ca^{2+}-activated CaM. In the case of SAP102, CaM binding has been shown to promote the formation of CaM-dependent heteromeric MAGUK protein complexes (24). CaM binding to SAP97 could have a similar function by relieving SH3 domain interference with the GK domain-GKAP interaction (21). In fact, modulation of the intramolecular SH3-GK interaction has been proposed as a general mechanism for regulating the clustering of the Kv1.4 potassium channel by SAP90 (28). However, the effect of the SH3 domain on the interaction of BEGAIN and GAKIN with the GK domain has not been evaluated yet. Also, full-length PSD-93/chapsyn-110 does not bind microtubule-associated protein 1A (MAP1A) as effectively as the isolated GK domain (15), the underlying mechanism being unclear. Preferential binding of CaM to a closed SAP97 conformation might affect the interactions of the GK domain and serve as a general negative regulator. In particular, because a role for SAP97 in the initial delivery of D-2-amino-3-hydroxy-5-methyl-4-isoxazole-propionic acid (AMPA) receptors to the synaptic membrane has recently been suggested (7), the interaction of CaM with SAP97 could disrupt the SAP97-motor protein interaction at synaptic membranes and facilitate initial glutamate receptor subunit 1 delivery.

In summary, our work shows that the CaM binding domain of SAP97 shares no, or only very low, sequence identity with other CaM target proteins, but it comprises a stretch of about 20–25 amino acid residues that have the potential to fold into a positively charged amphipathic α-helix, which forms the CaM recognition motif. Kinetic analysis of the interaction between CaM and SH3-HOOK-GK classifies SAP97 as a $(Ca^{2+})_4$·CaM target protein that binds with low to intermediate affinity. Although this work defines essential elements for binding of CaM, it is not yet clear how CaM affects the conformational state of SAP97. Because the SH3 and GK domains of SAP97 play a role in both intramolecular and intermolecular associations, the activation of SAP97 most likely occurs upon translocation from the cytosol to the plasma membrane and engagement of the SH3/GK domains by associating with glutamate receptor subunits. The key challenge will now be to translate the *in vitro* observations on CaM-SAP97 interaction to the regulatory mechanisms acting on the intact SAP97 molecule.

Acknowledgment—We thank Dieter Gallwitz for continuous support.

REFERENCES

1. Fanning, A. S., and Anderson, J. M. (1998) *Curr. Top. Microbiol. Immunol.* **228,** 209–233
2. O'Brien, R. J., Lau, L. F., and Huganir, R. L. (1998) *Curr. Opin. Neurobiol.* **8,** 364–369
3. Garner, C. C., Nash, J., and Huganir, R. L. (2000) *Trends Cell Biol.* **10,** 274–280
4. Hata, Y., Nakanishi, H., and Takai, Y. (1998) *Neurosci. Res.* **32,** 1–7
5. Muller, B. M., Kistner, U., Veh, R. W., Cases-Langhoff, C., Becker, B., Gundelfinger, E. D., and Garner, C. C. (1995) *J. Neurosci.* **15,** 2354–2366
6. Valtschanoff, J. G., Burette, A., Davare, M. A., Leonard, A. S., Hell, J. W., and Weinberg, R. J. (2000) *Eur. J. Neurosci.* **12,** 3605–3614
7. Sans, N., Racca, C., Petralia, R. S., Wang, Y. X., McCallum, J., and Wenthold, R. J. (2001) *J. Neurosci.* **21,** 7506–7516
8. Hibino, H., Inanobe, A., Tanemoto, M., Fujita, A., Doi, K., Kubo, T., Hata, Y., Takai, Y., and Kurachi, Y. (2000) *EMBO J.* **19,** 78–83
9. Sheng, M., and Sala, C. (2001) *Annu. Rev. Neurosci.* **24,** 1–29
10. Garcia, E. P., Mehta, S., Blair, L. A., Wells, D. G., Shang, J., Fukushima, T., Fallon, J. R., Garner, C. C., and Marshall, J. (1998) *Neuron* **21,** 727–739
11. Nix, S. L., Chishti, A. H., Anderson, J. M., and Walther, Z. (2000) *J. Biol. Chem.* **275,** 41192–41200
12. Kim, E., Naisbitt, S., Hsueh, Y. P., Rao, A., Rothschild, A., Craig, A. M., and Sheng, M. (1997) *J. Cell Biol.* **136,** 669–678
13. Satoh, K., Yanai, H., Senda, T., Kohu, K., Nakamura, T., Okumura, N., Matsumine, A., Kobayashi, S., Toyoshima, K., and Akiyama, T. (1997) *Genes Cells* **2,** 415–424
14. Takeuchi, M., Hata, Y., Hirao, K., Toyoda, A., Irie, M., and Takai, Y. (1997) *J. Biol. Chem.* **272,** 11943–11951
15. Brenman, J. E., Topinka, J. R., Cooper, E. C., McGee, A. W., Rosen, J., Milroy, T., Ralston, H. J., and Bredt, D. S. (1998) *J. Neurosci.* **18,** 8805–8813
16. Deguchi, M., Hata, Y., Takeuchi, M., Ide, N., Hirao, K., Yao, I., Irie, M., Toyoda, A., and Takai, Y. (1998) *J. Biol. Chem.* **273,** 26269–26272
17. Hanada, T., Lin, L., Tibaldi, E. V., Reinherz, E. L., and Chishti, A. H. (2000) *J. Biol. Chem.* **275,** 28774–28784
18. Kuhlendahl, S., Spangenberg, O., Konrad, M., Kim, E., and Garner, C. C. (1998) *Eur. J. Biochem.* **252,** 305–313
19. Li, Y., Spangenberg, O., Paarmann, I., Konrad, M., and Lavie, A. (2002) *J. Biol. Chem.* **277,** 4159–4165
20. Wu, H., Reuver, S. M., Kuhlendahl, S., Chung, W. J., and Garner, C. C. (1998) *J. Cell Sci.* **111,** 2365–2376
21. Wu, H. J., Reissner, C., Kuhlendahl, S., Coblentz, B., Reuver, S., Kindler, S., Gundelfinger, E. D., and Garner, C. C. (2000) *EMBO J.* **19,** 5740–5751
22. Marfatia, S. M., Byron, O., Campbell, G., Liu, S. C., and Chishti, A. H. (2000) *J. Biol. Chem.* **275,** 13759–13770
23. Lue, R. A., Marfatia, S. M., Branton, D., and Chishti, A. H. (1994) *Proc. Natl. Acad. Sci. U. S. A.* **91,** 9818–9822
24. Masuko, N., Makino, K., Kuwahara, H., Fukunaga, K., Sudo, T., Araki, N., Yamamoto, H., Yamada, Y., Miyamoto, E., and Saya, H. (1999) *J. Biol. Chem.* **274,** 5782–5790
25. O'Neil, K. T., and DeGrado, W. F. (1990) *Trends Biochem. Sci* **15,** 59–64
26. Rhoads, A. R., and Friedberg, F. (1997) *FASEB J.* **11,** 331–340
27. McGee, A. W., and Bredt, D. S. (1999) *J. Biol. Chem.* **274,** 17431–17436
28. Shin, H. W., Hsueh, Y. P., Yang, F. C., Kim, E., and Sheng, M. (2000) *J. Neurosci.* **20,** 3580–3587
29. Tavares, G., Panepucci, E., and Brunger, A. (2001) *Mol. Cell* **8,** 1313–1325
30. Lisman, J. E., and Zhabotinsky, A. M. (2001) *Neuron* **31,** 191–201
31. Husi, H., Ward, M. A., Choudhary, J. S., Blackstock, W. P., and Grant, S. G. (2000) *Nat. Neurosci.* **3,** 661–669
32. Yoshimura, Y., Shinkawa, T., Taoka, M., Kobayashi, K., Isobe, T., and Yamauchi, T. (2002) *Biochem. Biophys. Res. Commun.* **290,** 948–954
33. Woods, D. F., Hough, C., Peel, D., Callaini, G., and Bryant, P. J. (1996) *J. Cell Biol.* **134,** 1469–1482
34. Brundiers, R., Lavie, A., Veit, T., Reinstein, J., Schlichting, I., Ostermann, N., Goody, R. S., and Konrad, M. (1999) *J. Biol. Chem.* **274,** 35289–35292
35. Gill, S. C., and von Hippel, P. H. (1989) *Anal. Biochem.* **182,** 319–326
36. Karlsson, R., and Falt, A. (1997) *J. Immunol. Methods* **200,** 121–133
37. Persechini, A., and Cronk, B. (1999) *J. Biol. Chem.* **274,** 6827–6830
38. Jurado, L. A., Chockalingam, P. S., and Jarrett, H. W. (1999) *Physiol. Rev.* **79,** 661–682
39. Persechini, A., Stemmer, P. M., and Ohashi, I. (1996) *J. Biol. Chem.* **271,** 32217–32225
40. Gilli, R., Lafitte, D., Lopez, C., Kilhoffer, M., Makarov, A., Briand, C., and Haiech, J. (1998) *Biochemistry* **37,** 5450–5456
41. Chin, D., and Means, A. R. (2000) *Trends Cell Biol.* **10,** 322–328
42. DeMarco, S. J., and Strehler, E. E. (2001) *J. Biol. Chem.* **276,** 21594–21600
43. McGee, A. W., Dakoji, S. R., Olsen, O., Bredt, D. S., Lim, W. A., and Prehoda, K. E. (2001) *Mol. Cell* **8,** 1291–1301
44. Strynadka, N. C., and James, M. N. (1990) *Proteins* **7,** 234–248
45. Smith, C. W., Pritchard, K., and Marston, S. B. (1987) *J. Biol. Chem.* **262,** 116–122
46. Burns, N. R., and Gratzer, W. B. (1985) *Biochemistry* **24,** 3070–3074
47. Moarefi, I., LaFevre-Bernt, M., Sicheri, F., Huse, M., Lee, C. H., Kuriyan, J., and Miller, W. T. (1997) *Nature* **385,** 650–653
48. Evenas, J., Malmendal, A., and Forsen, S. (1998) *Curr. Opin. Chem. Biol.* **2,** 293–302
49. Lee, S. H., and Sheng, M. (2000) *Curr. Opin. Neurobiol.* **10,** 125–131
50. BIAtechnology Handbook (1998) version AB, pp. 5-1–5-9, Biacore AB, Uppsala, Sweden

PROTEIN STRUCTURE AND FOLDING:

Formation of Complexes between Ca^{2+}·Calmodulin and the Synapse-associated Protein SAP97 Requires the SH3 Domain-Guanylate Kinase Domain-connecting HOOK Region

Ingo Paarmann, Oliver Spangenberg, Arnon Lavie and Manfred Konrad

J. Biol. Chem. 2002, 277:40832-40838.
doi: 10.1074/jbc.M205618200 originally published online August 19, 2002